2230

Hippocampal Single-Voxel MR Spectroscopy with Long Echo Time at 3 Tesla

Martin Gajdošík[1,2], Karl Landheer[1], Kelley M. Swanberg[1], Fatemeh Adlparvar[2], Guillaume Madelin[2], Wolfgang Bogner[3], Christoph Juchem[1,4], and Ivan I. Kirov[2,5,6]
[1]Department of Biomedical Engineering, Columbia University, New York City, NY, United States, [2]Bernard and Irene Schwartz Center for Biomedical Imaging, Department of Radiology, New York University Grossman School of Medicine, New York City, NY, United States, [3]High-Field MR Center, Department of Biomedical Imaging and Image-Guided Therapy, Medical University of Vienna, Vienna, Austria, [4]Department of Radiology, Columbia University Medical Center, New York City, NY, United States, [5]Department of Neurology, New York University Grossman School of Medicine, New York City, NY, United States, [6]Center for Advanced Imaging Innovation and Research, Department of Radiology, New York University Grossman School of Medicine, New York City, NY, United States

Synopsis

The hippocampus is one of the most challenging brain regions for proton MR spectroscopy (MRS) applications. Moreover, quantification of *J*-coupled species such as myo-inositol (m-Ins) and glutamate + glutamine (Glx) is affected by the presence of macromolecular background. Here we investigate the feasibility of reproducibly measuring their concentrations at long T_E of 120 ms, using sLASER localization.

Introduction

The hippocampus is one of the most challenging brain regions for obtaining reliable MRS data. Short echo time MRS (T_E < 50 ms) is generally preferred due to increased SNR and limited *J*-evolution (i.e. signal complication) of metabolites[1]. However, resolving spectral overlap at short T_E remains a challenge, and the optimal way to report systematic error sources such as the macromolecular (MM) background is still under debate[2]. The effective T_2 relaxation times of 10 different macromolecular resonances were recently reported, enabling the selection of the shortest possible T_E at which the MM background has decayed to the noise level[3] (Figure 1).

The two objectives of this work were:

1. to minimize chemical shift displacement errors and minimize macromolecular background by employing a semi-adiabatic localization by adiabatic selective refocusing (sLASER) sequence[4] with 120 ms T_E.
2. to establish the signal variability of the resulting long-T_E sLASER approach in terms of coefficients of variation (CVs) of metabolite concentrations.

Methods

Subjects & Hardware

Six subjects (3 males; mean ± standard deviation 32.5 ± 10.2 years)) were scanned as follows: three (1 male) at the Center for Biomedical Imaging (CBI) at New York University Langone Health, and three (2 males) at the Jerome L. Greene Science Center at Columbia University, part of the Columbia MR Research Center (CMRRC). All subjects were scanned in Siemens Prisma 3 T systems (Siemens Healthineers, Erlangen, Germany) using a standard clinical 20-channel head coil (Siemens).

MRI, MRS & Data processing

Hippocampi were localized to a 3.4-mL VOI (26x10x13 mm^3) in left hippocampus referencing 3D MP-RAGE sequence. VOI brain tissue was segmented from the resultant images with SPM12[5]. Metabolites were measured using sLASER with an optimized sinc excitation pulse and four GOIA-W(16,4) refocusing pulses (6) (T_E = 120 ms, T_R = 1.5 s, number of excitations = 256 with 4 dummy scans). All spectra were acquired as 2048 complex points, with a spectral bandwidth of 2000 Hz and 32-step phase cycling[7]. Spectral processing and linear combination modeling with a MARSS-simulated[8,9] basis set (myi-inositol: m-Ins, scyllo-inositol: s-Ins, choline-containing compounds: Cho, creatine: Cr, glutamine: Gln, glutamate: Glu, N-acetyl aspartate: NAA and lactate: Lac) were done in INSPECTOR[10–12]. Since several amino acids resonate close to the signal of lactate[13], detected signal from this frequency range was termed Lac+. Sum of Glu and Gln was termed Glx. Fit parameter precision was estimated with Cramér-Rao lower bounds (CRLB)[14]. Absolute metabolite concentrations were calculated using the measured water signal[15], taking into account published water and metabolic relaxation times[16–22].

Signal variability

Variability of metabolite concentrations within sessions, within subjects, and between subjects were assessed with coefficients of variation (CV), defined as the ratio of the standard deviation to the mean. “Within-session” refers to variability among three consecutive scans in one session of the same subject. “Within-subject” was defined as variability between the first scan from both distinct sessions in the same subject. “Between-subject” was defined as variability among all subject scans, where subject scan was defined as only the first scan from the first session. Overview of the experimental setup and illustration of calculation of the three variances is shown in Figure 2. Metabolite concentrations for all subjects were reported from session #1 and scan #1.

Results & Discussion

Voxel placement for the left hippocampus is shown in Figure 3A. A hippocampal spectrum acquired at 120 ms T_E is shown with its fitted linear combination model in Figure 3B and basis set for quantification in Figure 3C. Mean metabolite concentrations (reported from session #1 and scan #1) from all subjects measured at both sites are summarized with their corresponding mean CRBLs in Table 1.

The within-session CVs ranged from low values for NAA (across all six subjects: session one 3.5 ± 1.4%; session two 2.2 ± 1.6%) to high values for s-Ins (62.3 ± 59.8%; 56.6 ± 59.8%, respectively). The within-session CVs of all basis set metabolites are shown in Table 2A. Within-subject CVs ranged from a minimum of 0.6% for NAA in subject #6 to a maximum of 141.4% for s-Ins in the same subject (Table 2B). Between-subject CVs of volume fractions and metabolite concentrations from session 1 and scan 1 of all subjects are summarized in Table 2C.

Conclusion

We showed that presented sLASER sequence can be used to reliably measure metabolites in the hippocampus, a key region affected in many neurological disorders, using the shortest T_E at which macromolecules have been shown in cortical regions to decay to the noise level. We report the CVs of all major metabolites including Glx and m-Ins to inform sample size estimations for future studies of the hippocampus in which the presence of MM baseline is undesirable.

Acknowledgements

This study was funded by the National Institutes of Health (NIH) through the following grants: P30AG008051, R21NS112853 and P41EB017183. This work was performed at the Center for Biomedical Imaging at New York University Langone Health and at the Zuckerman Mind Brain Behavior Institute MRI Platform, a shared resource.

References

1. Landheer K, Gajdošík M, Juchem C. A semi-LASER, single-voxel spectroscopic sequence with a minimal echo time of 20.1 ms in the human brain at 3 T. NMR Biomed. 2020:e4324 doi: 10.1002/nbm.4324.

2. Giapitzakis I, Borbath T, Murali-Manohar S, Avdievich N, Henning A. Investigation of the influence of macromolecules and spline baseline in the fitting model of human brain spectra at 9.4T. Magn. Reson. Med. 2019;81:746–758 doi: 10.1002/mrm.27467.

3. Landheer K, Gajdošík M, Treacy M, Juchem C. Concentration and effective T2 relaxation times of macromolecules at 3T. Magn. Reson. Med. 2020:mrm.28282 doi: 10.1002/mrm.28282.

4. Scheenen TWJ, Klomp DWJ, Wijnen JP, Heerschap A. Short echo time 1H-MRSI of the human brain at 3T with minimal chemical shift displacement errors using adiabatic refocusing pulses. Magn. Reson. Med. 2008;59:1–6 doi: 10.1002/mrm.21302.

5. Ashburner J, Friston KJ. Unified segmentation. Neuroimage 2005;26:839–851 doi: 10.1016/j.neuroimage.2005.02.018.

6. Andronesi OC, Ramadan S, Ratai E, Jennings D. Spectroscopic Imaging with Improved Gradient Modulated Constant Adiabaticity Pulses on High-Field Clinical Scanners. J Magn Reson 2010;203:283–293 doi: 10.1016/j.jmr.2010.01.010.Spectroscopic.

7. Neji R, Schuster C. Phase Cycling for Semi-Laser Single Voxel Spectroscopy. In: Proceedings of Annual Meeting of International Society for Magnetic Resonance in Medicine. ; 2014. p. 3723.

8. Landheer K, Juchem C. Magnetic Resonance Spectrum Simulator - MARSS. http://innovation.columbia.edu/technologies/CU19215_MARSS.

9. Landheer K, Swanberg KM, Juchem C. Magnetic resonance Spectrum simulator (MARSS), a novel software package for fast and computationally efficient basis set simulation. NMR Biomed. 2019:1–13 doi: 10.1002/nbm.4129.

10. Juchem C. INSPECTOR: Magnetic resonance spectroscopy software for optimized data extraction. innovation.columbia.edu/technologies/cu17130_inspector. Published 2020.

11. Juchem C. INSPECTOR: "The New Kid on the Block." ISMRM Virtual Study Group Meeting - MR Spectroscopy. https://ismrm.adobeconnect.com/_a1156337412/pvzkfszv1l4s/. Published 2017.

12. Gajdošík M, Landheer K, Swanberg KM, Juchem C. INSPECTOR: Free Software for Magnetic Resonance Spectroscopy Data Inspection, Processing, Simulation and Analysis. Sci. Rep.:In revision.

13. Grand S, Passaro G, Ziegler A, et al. Necrotic Tumor versus Brain Abscess: Importance of Amino Acids Detected at 1 H MR Spectroscopy—Initial Results. Radiology 1999;213:785–793 doi: 10.1148/radiology.213.3.r99dc10785.

14. Cavassila S, Deval S, Huegen C, Van Ormondt D, Graveron-Demilly D. Cramer-Rao Bound Expressions for Parametric Estimation of Overlapping Peaks: Influence of Prior Knowledge. J. Magn. Reson. 2000;143:311–320 doi: 10.1006/jmre.1999.2002.

15. Brief EE, Moll R, Li DKB, MacKay AL. Absolute metabolite concentrations calibrated using the total water signal in brain 1 H MRS. NMR Biomed. 2009;22:349–354 doi: 10.1002/nbm.1349.

16. Lu H, Nagae-Poetscher LM, Golay X, Lin D, Pomper M, van Zijl PCM. Routine clinical brain MRI sequences for use at 3.0 Tesla. J. Magn. Reson. Imaging 2005;22:13–22 doi: 10.1002/jmri.20356.

17. Terpstra M, Cheong I, Lyu, Tianmeng L, et al. Test-retest reproducibility of neurochemical profiles with short-echo, single voxel MRS at 3T and 7T. Magn Reson Med 2016;76:1083–1091 doi: 10.1016/j.physbeh.2017.03.040.

18. Deelchand DK, Adanyeguh IM, Emir, U E, et al. Two-site reproducibility of cerebellar and brainstem neurochemical profiles with short-echo, single voxel MRS at 3 T. Magn Reson Med 2015;73:1718–1725 doi: 10.1016/j.physbeh.2017.03.040.

19. Ernst T, Kreis R, Ross BD. Absolute Quantitation of Water and Metabolites in the Human Brain. I. Compartments and Water. J. Magn. Reson. Ser. B 1993;102:1–8 doi: 10.1006/jmrb.1993.1055.

20. Mlynarik V, Gruber S, Moser E. Proton T1 and T2 relaxation times of human brain metabolites at 3 Tesla. NMR Biomed. 2001;14:325–331 doi: 10.1002/nbm.713.

21. Wyss PO, Bianchini C, Scheidegger M, et al. In vivo estimation of transverse relaxation time constant (T 2) of 17 human brain metabolites at 3T. Magn. Reson. Med. 2018;80:452–461 doi: 10.1002/mrm.27067.

22. Allaïli N, Valabrègue R, Auerbach EJ, et al. Single-voxel 1 H spectroscopy in the human hippocampus at 3 T using the LASER sequence: characterization of neurochemical profile and reproducibility. NMR Biomed. 2015;28:1209–1217 doi: 10.1002/nbm.3364.

23. Wyss PO, Huber E, Curt A, Kollias S, Freund P, Henning A. MR Spectroscopy of the Cervical Spinal Cord in Chronic Spinal Cord Injury. Radiology 2019:181037 doi: 10.1148/radiol.2018181037.

Figures

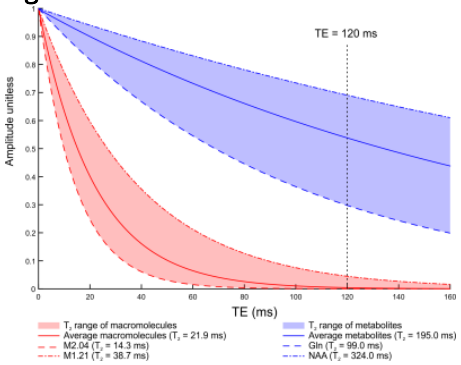

Figure 1: Simplified simulations of T_2 relaxation of normalized signals for macromolecules (MM) and metabolites. The average T_2 relaxation times and ranges of macromolecules and metabolites were calculated from literature[3,14,15]. Note that at T_E = 120 ms, most MM signal is gone, while on average 60% of the metabolite signal remains. This demonstrates that relatively little metabolite signal was lost while the specific choice of T_E = 120 ms enabled easily quantifiable Glu+Gln (Glx)) and m-Ins resonances.

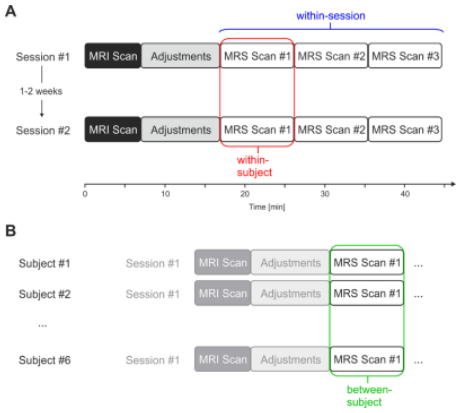

Figure 2: Experimental details. (A) All experimental measurements for one subject and illustrations of data used for calculation of within-session and within-subject variability. (B) Illustration of data used for calculation of between-subject variability.

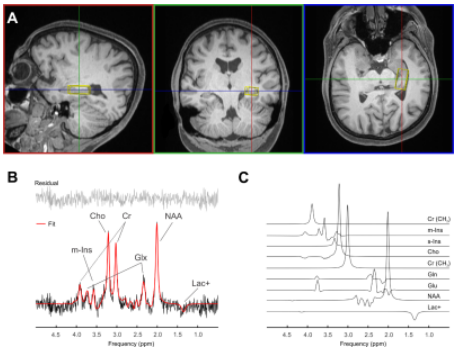

Figure 3: MRS acquisition and spectral analysis. (A) Placement of the 3.4 mL voxel (26 x 10 x 13 mm^3) in the left hippocampus (52 years, woman), containing mainly its body and tail. (B) Spectrum from the hippocampus fitted with linear combination modelling. Note, no macromolecular background in the residual signal. (C) Basis set used for quantification of hippocampal metabolites.

Site			m-Ins	s-Ins	Cho	Cr	Gln	Glu	Glx	NAA	Lac+
CBI	Concentration	Mean	5	0.6	1.6	5.7	2	9.2	11.2	5.9	2.6
		S.D.	2	0.2	0.2	0.4	1.3	2.4	1.8	0.5	0.6
	CRLB	Mean	10.4	35.6	6.4	3.8	32.1	11.4	-	2.2	15.7
		S.D.	6.1	24.2	1.7	0.6	27.2	1.8	-	0.3	3.5
CMRRC	Concentration	Mean	5.8	0.4	1.8	5.9	2.7	9.2	11.9	5.9	2.4
		S.D.	0.5	0.4	0.3	0.3	0.8	1.1	0.4	0.3	0.9
	CRLB	Mean	24.8	70.8	8.2	4.9	22.9	12.5	-	2.6	30.9
		S.D.	8.4	35	3.8	0.3	12.1	1.2	-	0.3	26.2
All	Concentration	Mean	5.4	0.5	1.7	5.8	2.4	9.2	11.6	5.9	2.5
		S.D.	1.4	0.3	0.2	0.3	1	1.7	1.2	0.4	0.7
	CRLB	Mean	20.6	59.7	7.3	4.3	27.5	12	-	2.4	23.3
		S.D.	8	34.8	2.8	0.6	19.5	1.5	-	0.4	18.7

Table 1: Metabolite concentrations (mM), standard deviations (S.D.) and Cramér-Rao Lower Bounds (CRLBs in %) of all subjects from Session #1 and Scan #1, measured at two different sites.

A Within-session coefficients of variation [%]

		m-Ins	s-Ins	Cho	Cr	Gln	Glu	Glx	NAA	Lac+
Sub. #1	Sess. #1	13.8	39.6	2.1	6.4	30.7	13.6	4.4	1.5	7.7
	Sess. #2	4.9	38.4	4.4	4.4	24	2	4.2	1.5	14.9
Sub. #2	Sess. #1	6.2	18.9	9.9	4.9	28.9	22.1	19.6	4.3	33.1
	Sess. #2	18.9	64.1	2.3	9.4	66.1	9.7	17.9	4.2	47.6
Sub. #3	Sess. #1	19.3	10.1	2.1	2.7	8.9	16.2	12.9	2.9	20.2
	Sess. #2	33.7	31.6	8.3	2.8	33.1	12.8	14	0.7	16.1
Sub. #4	Sess. #1	9.8	87.3	5.6	4.4	12.7	3.2	3	4.5	33.4
	Sess. #2	22.7	18	2	2.9	21.2	4.5	6.2	1.5	19.9
Sub. #5	Sess. #1	16	46.4	15.4	5.4	4.5	15.6	13.9	5.3	7.5
	Sess. #2	26.3	14.5	6	11.6	20.8	13.6	9.8	4.1	6.8
Sub. #6	Sess. #1	22	171.3	3.5	12.4	14.1	9.3	9.5	2.4	33.2
	Sess. #2	25.7	173.2	8	11.5	30.5	7.3	10.8	0.9	57.9
Mean	Sess. #1	14.5	62.3	6.5	6	16.3	13.3	10.6	3.5	22.5
S.D.		5.9	59.8	5.3	3.4	11.1	6.5	6.2	1.4	12.6
Mean	Sess. #2	22	56.6	5.2	7.1	32.6	8.3	10.5	2.2	27.2
S.D.		9.7	59.8	2.7	4.2	17.1	4.6	5	1.6	20.5

B Within-subject coefficients of variation [%]

	m-Ins	s-Ins	Cho	Cr	Gln	Glu	Glx	NAA	Lac+
Sub. #1	13.6	9.3	3	6.4	2.3	19.7	15.5	6	2.5
Sub. #2	4.7	40.7	2.6	4.2	37.4	16.2	17.3	4.3	7.2
Sub. #3	7.4	19.1	9.4	8.5	2.4	6.3	5.1	3	22.8
Sub. #4	28.4	75.6	1.2	4.7	33.2	1.7	6.4	5.8	12.4
Sub. #5	3.1	39.2	10.8	19.6	15.9	15.2	15.3	9.3	21.3
Sub. #6	59	141.4	17.7	1.1	7.2	18	15	0.6	83.1
Mean	17.8	52.7	7.5	7.4	16.4	12.8	12.4	4.8	24.9
S.D.	18.2	49.1	6.3	6.4	15.5	7.2	5.3	3	29.6

C Between-subject coefficients of variation [%]

m-Ins	s-Ins	Cho	Cr	Gln	Glu	Glx	NAA	Lac+
25	62.7	12.3	5.3	43.6	18	10.7	6.4	29.2

Table 2: A - Within-session coefficients of variation [%] calculated per subject (Sub.) and session (Sess.). B - Within-subject coefficients of variation [%] calculated per subject (Sub.). C - Between-subject coefficients of variation [%] calculated from session #1 and scan #1 of all subjects.

Proc. Intl. Soc. Mag. Reson. Med. 29 (2021)
2230